Supporting Information for

Room-Temperature Switching of Magnetic Hysteresis by Reversible Single-Crystal-to-Single-Crystal Solvent Exchange in Imidazole-Inspired Fe(II) Complex

Wei Huang,[a] Fuxing Shen,[a] Ming Zhang,[a] Dayu Wu,[a]* Feifei Pan,[a] and Osamu Sato[b]

[a] Jiangsu Key Laboratory of Advanced Catalytic Materials and Technology, Collaborative Innovation Center of Advanced Catalysis & Green Manufacturing, School of Petrochemical Engineering, Changzhou University, Changzhou, Jiangsu 213164, China;

[b] Institute for Materials Chemistry and Engineering, Kyushu University, 744 Motooka, Nishi-ku, Fukuoka, 819-0395, Japan.

Table S1. Summary of the Solvent- and Anion-Ligand Hydrogen Bond Parameters Found in **1**-Et_2O **and 1**-$3H_2O$.

complex	D-H	A	d(D-H)/Å	d(H…A)/Å	d(D…A)/Å	∠(DHA)/deg
1-Et_2O @298K	N2-H2B	F3	0.86	2.339	2.984	132.1
	N2-H2B	F1	0.86	2.254	2.821	123.41
	N2-H2B	F4	0.86	2.541	3.072	120.82
	N5-H5A	O2	0.86	2.236	3.085	169.22
	N6-H6A	F2	0.86	2.106	2.931	160.49
	N6-H6A	F4	0.86	2.342	3.053	140.22
1-Et_2O @120K	N2-H2B	F1	0.88	2.072	2.903	157.12
	N3-H3A	O3	0.88	2.16	3.024	167.19
	N7-H7B	F2	0.88	2.584	3.062	115.02
	N7-H7B	F3	0.88	2.321	3.014	135.67
	N7-H7B	F4	0.88	2.292	2.845	120.82
	N8-H8B	F5	0.88	2.113	2.741	127.7
	N8-H8B	F6	0.88	2.444	3.085	130.06
	N13-H13A	F7	0.88	1.982	2.835	162.94

complex	D-H	A	d(D-H)/Å	d(H…A)/Å	d(D…A)/Å	∠(DHA)/deg
1-$3H_2O$ @298K	C29-H29A	F7A_b	0.95	2.456	3.026	118.43
	N2-H2B	F2_a	0.88	2.108	2.958	162.11
	N2-H2B	F4A_b	0.88	2.191	2.887	135.7
	N6-H6B	F1	0.88	2.357	2.913	121.3
	N6-H6B	F3	0.88	2.356	3.043	134.97
	N6-H6B	F4_a	0.88	2.576	3.092	118.33
	N8-H8B	F5	0.88	2.053	2.91	164.4
	N10-H10A	O3W	0.88	2.219	3.084	167.55
	N14-H14B	F8_a	0.88	1.988	2.71	138.47
1-$3H_2O$ @120K	N1-H1B	F7	0.86	2.006	2.84	162.96
	N7-H7B	F5	0.86	2.359	2.991	130.69
	N7-H7B	F6	0.86	2.141	2.758	128.31
	N8-H8B	F4	0.86	2.062	2.88	158.77
	N14-H14B	F1	0.86	2.276	2.947	134.94
	N14-H14B	F2	0.86	2.332	2.884	122.25
	O1W-H1WA	F3	0.85	2.436	2.899	115.03
	O1W-H1WB	O3W	0.85	1.974	2.789	160.38
	O2W-H2WB	O1W	0.85	1.855	2.676	161.98
	O3W-H3WA	O4W	0.85	2.079	2.578	117.02

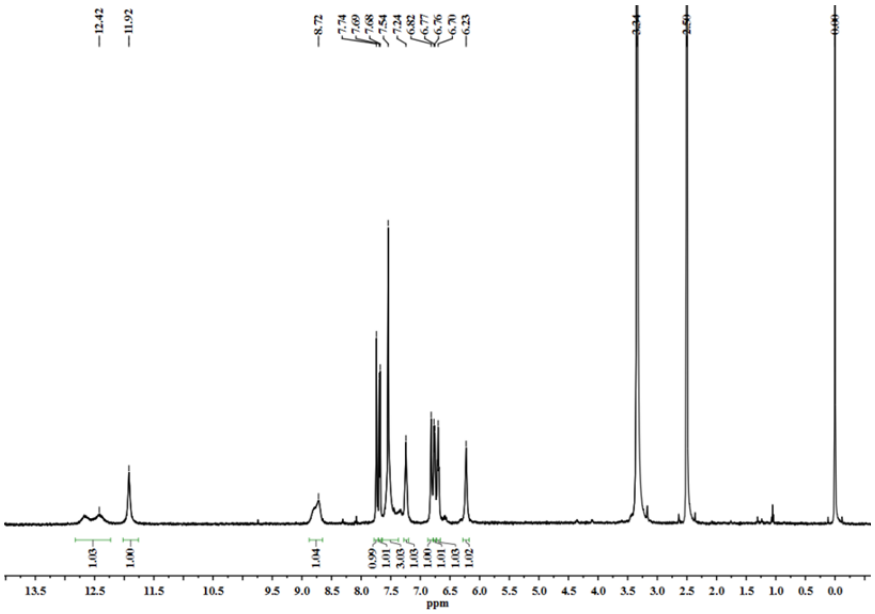

Figure S1. ^{1}H NMR spectrum of **Liq** in DMSO at room temperature.

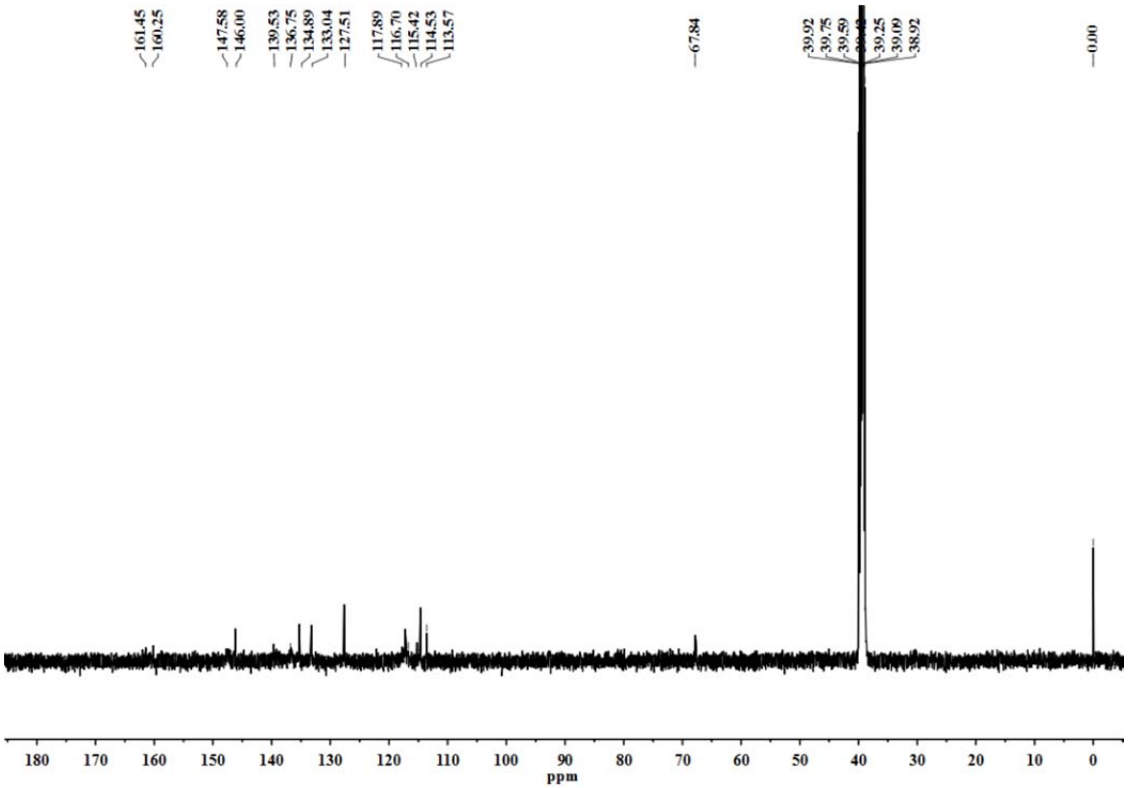

Figure S2. ^{13}C NMR spectrum of **Liq** in DMSO at room temperature.

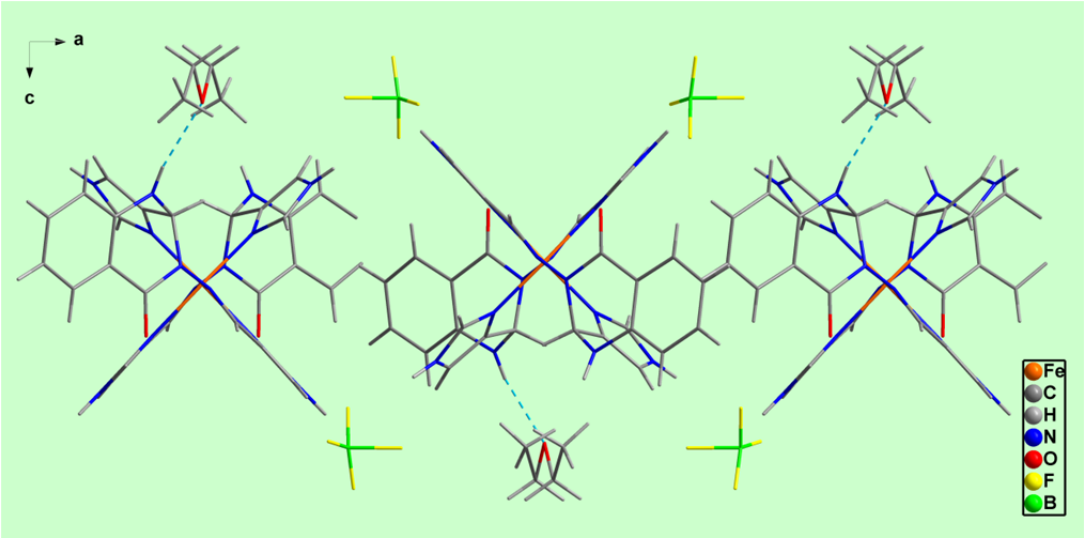

Figure S3. View of the hydrogen bonding interactions between O atoms of Et_2O and N on the ligand through N−H···O interactions in **1**-Et_2O.

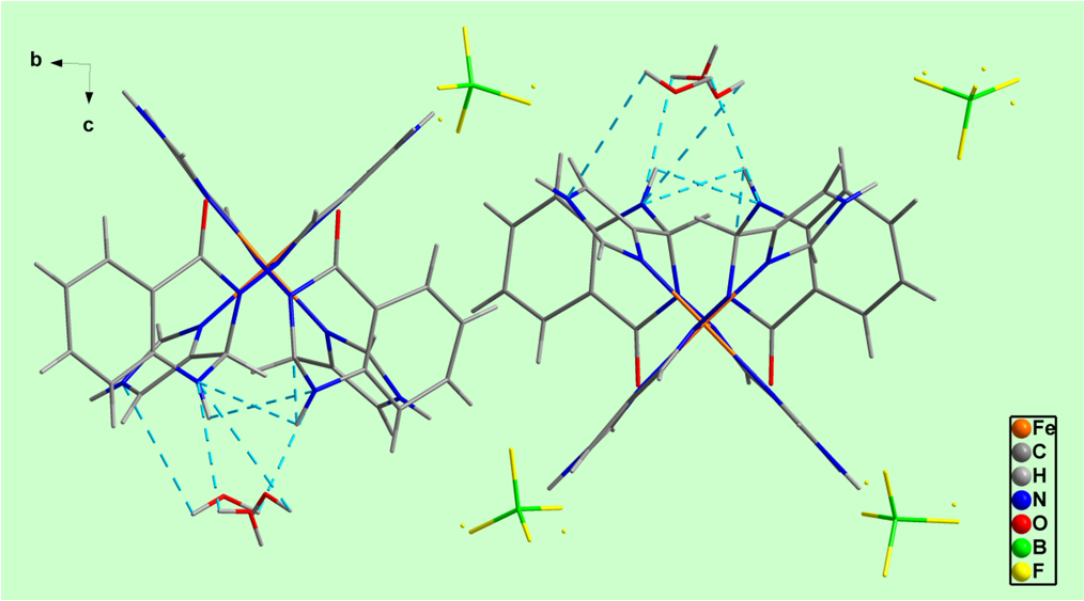

Figure S4. View of the hydrogen bonding interactions between O atoms of H_2O and N on the ligand through N−H···O interactions in **1**-$3H_2O$.

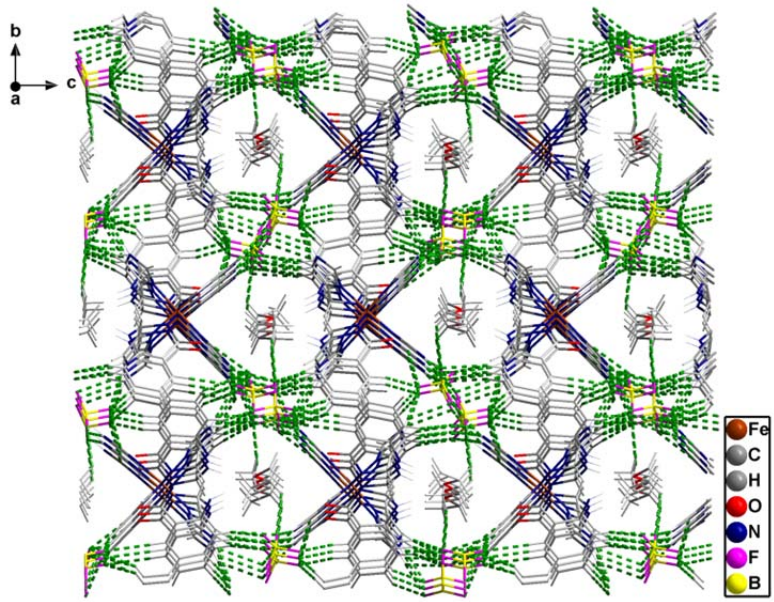

Figure S5. View of the supramolecular three-dimensional arrangement through N−H···F interactions in **1**-Et_2O at 298K.

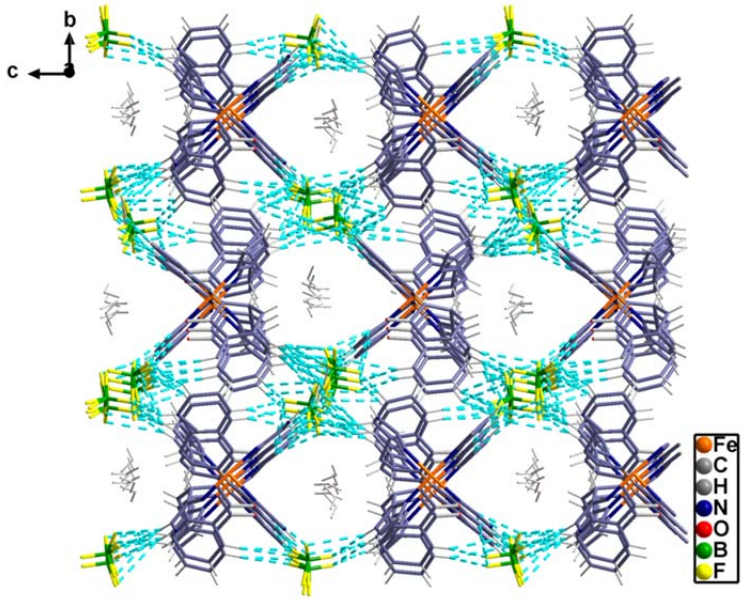

Figure S6. View of the supramolecular three-dimensional arrangement through N−H···F interactions in **1**-$3H_2O$ at 298K.

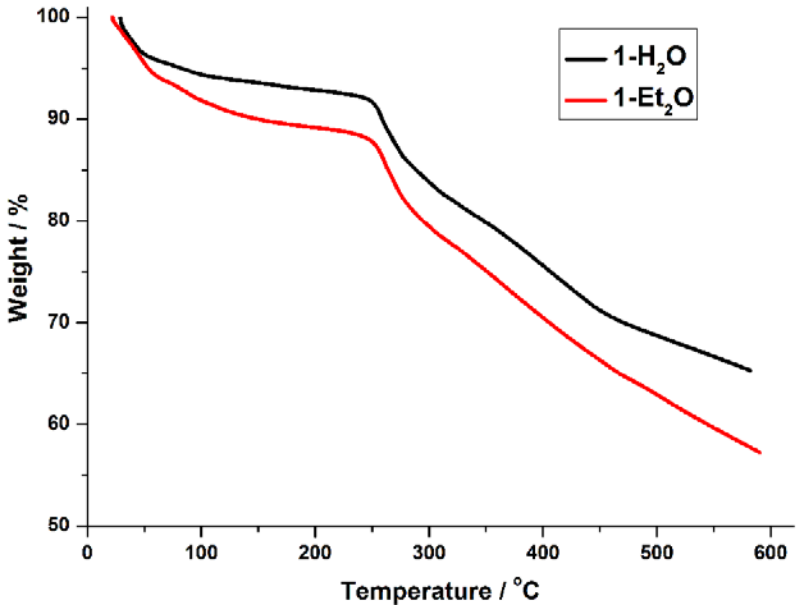

Figure S7. TG analysis of $[Fe(Liq)_2](BF_4)_2 \cdot C_4H_{10}O$ **(1**-Et_2O**)** and $[Fe(Liq)_2](BF_4)_2 \cdot H_2O$ **(1**-$3H_2O$**)**.

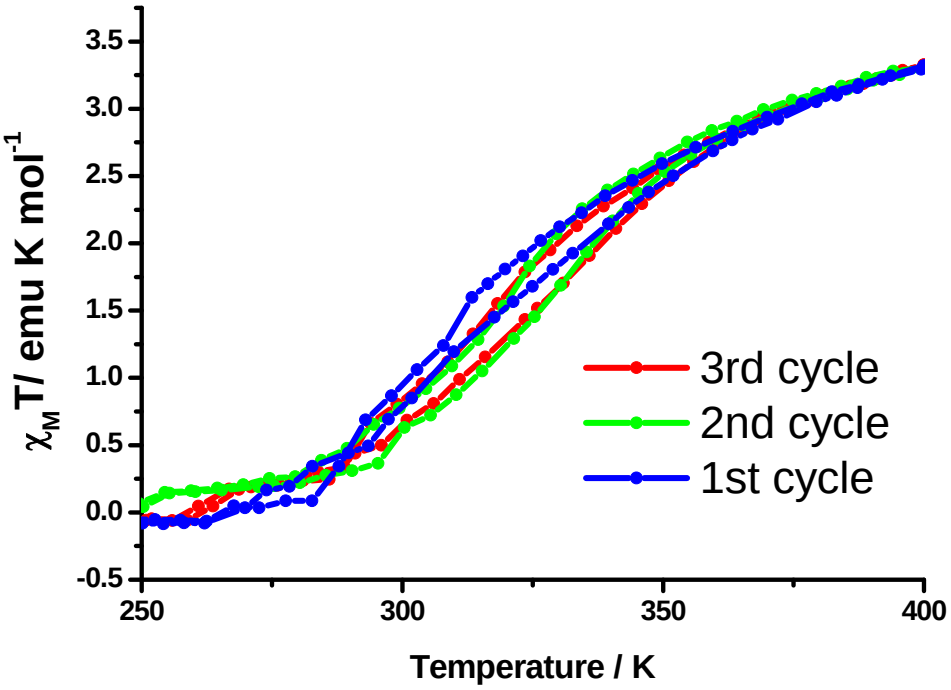

Figure S8. The magnetic data of sample **1**-Et_2O in the temperature range of 5-400 K.

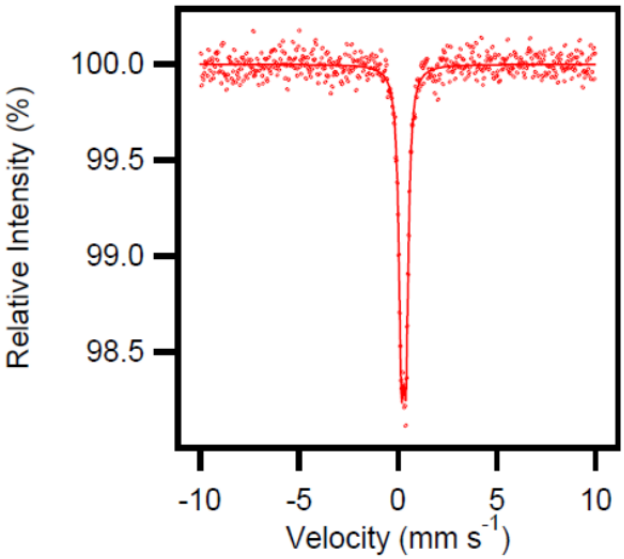

Figure S9. Mössbauer spectrum of complex **1**-3H_2O at 300 K.

Area: 100%

Isomer Shift: 0.300 (Standard Deviation 0.0026)

Quadrupole Splitting: 0.235 (Standard Deviation 0.0047)

Line Width: 0.299 (Standard Deviation 0.0081)

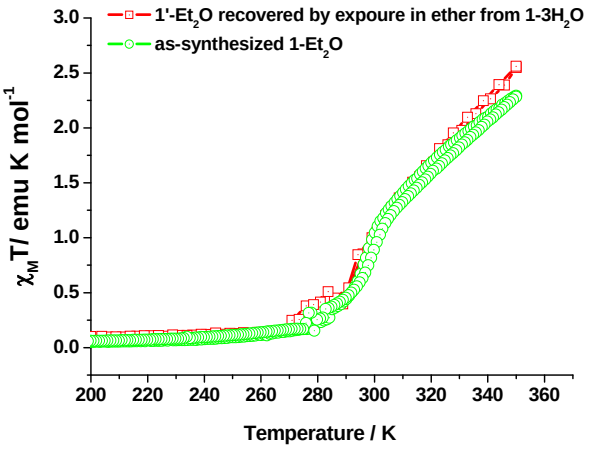

Figure S10. Variable-temperature magnetic susceptibility data of recovered sample **1**'-Et_2O which is exposed in Et_2O vapour by **1**-$3H_2O$ after 2 days and the comparison with the data of as-synthesized **1**-Et_2O.